

Simulating Materials in Nuclear Reactors

Colton Adamick Isaac Hoffman Anna Mast Sean Murray Kai Wells

Advisor: Prof. Jessica Krogstad
Course: MSE 395 Spring 2016

Mission

Mission Statement

Our mission is to simulate metals used in problematic areas of nuclear reactors to accelerate evaluation of suggested alternatives and develop an understanding of the difficulties and limitations of materials modeling.

Significance and Background

Many nuclear reactors in the U.S. are nearing the end of their original life expectancy. This raises questions on how to improve the longevity and reliability of existing and next generation nuclear reactors. It is inherently difficult to develop materials for use in the extreme environment of a reactor. Radiation involved with the production of nuclear power not only makes it unsafe for human contact, but also causes dramatic and unpredictable changes to material structure after very long exposure periods. This makes experimental research and development of suitable structural materials difficult. Simulation has therefore become an intriguing tool to determine the suitability of a material for extended use in the high temperature, pressure, and radiation of a nuclear reactor.

One simulation package that could be used for this purpose is the Multiphysics Object-Oriented Simulation Environment (MOOSE). MOOSE is an open source, finite-element, multiphysics framework developed by Idaho National Lab that can simulate materials over a range of length scales from near atomic to full scale multi-component systems. The framework uses adaptive finite element meshes and time stepping to reduce simulation time. These features, in addition to a wide variety of built-in physics models including phase field modelling, make MOOSE a good starting point for attempting non-trivial materials simulation.

Phase field modelling is a powerful technique for simulating microstructure evolution over long periods of time [1]. It treats composition and structure as a system of linear and nonlinear equations coupled by differential equations describing diffusion and other effects. Some quantities, such as atom concentration and density, are conserved while others, such as phase and grain count, are not conserved; such considerations are handled automatically by MOOSE. Phase field modelling can be used to solve the Cahn-Hilliard equation for phase separation. The Cahn-Hilliard equation relates the mobility and free energy gradient of each species with the time derivative of its composition. The equation has been used to simulate iron alloy decomposition.

During our visit to the Clinton Power Station in Clinton, IL we learned that stress corrosion cracking (SCC) of core shrouds is a problem in several reactors throughout the country. This served as the motivation for the simulations performed for this project. The core shroud is a large cylinder of 304 or 304L type stainless steel which surrounds the fuel rods within the reactor and directs the flow of water through the fuel rods for cooling and power production; its location in a reactor vessel is shown schematically in Figure A1. The core shroud consists of many welded plates, and SCC has been found in areas where welding has taken place [2]. SCC in these welds is mostly likely due to the depletion of Cr from grain boundaries after the formation of M₂₃C₆ carbides. We think these carbides could have formed due to welding side effects (i.e. sensitization of the heat affected zone) in combination

with radiation induced segregation of carbide forming elements to the grain boundaries [3]. If the cracking becomes severe enough that the shroud can no longer properly direct the flow of water in the reactor, catastrophic failure in the form of a reactor meltdown could occur, making the core shroud a critical component in maintaining a safe reactor.

Specific Objectives

Keeping in mind our mission statement and motivation for simulations, we had some specific objectives for the project. The first objective was to gain familiarity with the MOOSE framework and its advantages and disadvantages. This was done through the completion of two simple MOOSE tutorials: simulated Fe-Cr spinodal decomposition and simulated Cu grain growth. Our next objective was to gather necessary values for relevant simulation inputs by searching literature or making our own calculations. The final objective for this project was to use an existing MOOSE physics module to simulate changes in a material that was under the conditions found in a reactor environment for a long period of time. These simulations were performed for materials with a wide range of compositions similar to that of 304L steel.

Design Constraints

Constraint	Type	Quantification	Priority
Material must maintain suitable safety factor for expected lifetime	Physical	> 40 years	High
Ability to withstand high temperature and pressure for expected lifetime	Physical	570°F, 7 MPa	High
Reasonable computation requirements	Simulation	< 8 GB RAM	Med
Inability to combine multiple MOOSE modules	Simulation	N/A	Med
Cannot require regular maintenance	Physical	≤ once per year	Med
Material and fabrication cost must be within budget for a new plant	Financial	\$1-3B per plant	Low

Since the purpose of these simulations is to speed up approval of materials for use in nuclear reactors, several of the design constraints for this project relate to the physical properties of materials which are being simulated. If simulated materials do not meet these design constraints, they would not be suitable for use in the reactor. The lifetime, ability to withstand extreme environments, and limited maintenance interval all constrain the simulations of potential alternative materials for this project to metals which are similar to that which is already used.

Another important constraint concerns the simulation itself rather than what is being simulated. Due to limited resources, the computational requirements for running the simulation must be reasonable for a personal computer to execute. This limited our simulation size to 8GB of RAM. Due to adaptive time stepping, total simulated time was not a constraint on computation execution time.

Combining SCC, phase stability, and neutron radiation into a single simulation is very complex. In MOOSE, models for microstructural effects and elemental diffusion are separate modules. While we could easily model individual effects such as spinodal decomposition and grain evolution, it was not clear how to combine them to work together. For this reason, we chose to constrain the scope of our simulation to chemical segregation of a Fe-Ni-Cr system at various compositions.

Finally, in order for an alternate material to be feasible for use it must fit within the budget for building a new reactor. Due to the large budgets associated with the building of a nuclear plant and the relatively small difference in cost between different stainless steels, this constraint is not of great concern for this project.

Final Design Concept

Our final design for this project consisted of using the Cahn-Hilliard model to investigate how varying the Cr and Ni compositions of a 304L stainless steel affects the segregation of each alloying element over a 100 year timeframe at the temperatures and pressures experienced inside of a boiling water reactor. The Cahn-Hilliard model requires local free energies and composition-dependent mobilities as inputs to predict chemical segregation; Thermo-Calc and equations from the Saito paper [4] were used to provide these quantities, respectively. This design does not address neutron radiation damage, but could be expanded to do so if equations describing changes in free energy due to vacancy generation were identified. This design is shown schematically in Figure 1. The intended outcome of performing these simulations was to see if we could vary the composition of stainless steels to affect the chemical stability of the alloy at relevant conditions.

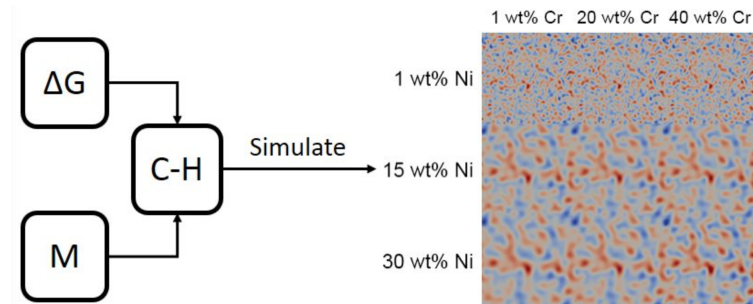


Figure 1: The final design involved finding composition-dependent equations for the free energy (ΔG) and mobility (M) of each variable species, feeding these into a Cahn-Hilliard (C-H) model, and simulating the composition distribution change over 100 years. The results could then be compared across a range of compositions to draw conclusions about the optimal alloy composition.

It was decided to use a modified version of the MOOSE Fe-Cr Cahn-Hilliard model tutorial, increasing from two species to three to reflect the addition of Ni to the system. Ni and Cr were chosen as the variable species because they are the majority alloying elements and could have the biggest impact on the stability of the γ -austenite, which could assist in the formation of carbides and other detrimental constituents such as topologically close packed phases. Other notable physical phenomenon, such as radiation effects, and SCC behavior of the HAZ were considered as additional points of interest, but the MOOSE documentation concerning these was limited. Due to these limitations, the overall complexity and scope of the final simulation design was vastly reduced throughout our design process.

For use in the Cahn-Hilliard model, free energy values for Ni and Cr in steels with compositions as described in Table A1 were obtained using Thermo-Calc. The amount of Ni and Cr were varied between 0.01 and 40 wt% with data collected at increments of 5 wt%. The rationale for the ranges chosen for Ni and Cr composition was two-fold. Firstly, these ranges are centered on a typical 304L composition of 20 wt% Cr and 10 wt% Ni. Secondly, accuracy in the free energy landscape over a wide range was necessary to take into account the potentially dramatic chemical segregation induced by radiation, processing, or welding. Free energies beyond this range were disregarded due to the fact that materials with such large compositions of Ni and Cr are no longer steels.

These free energy values were fit to a fifth order two-dimensional polynomial to produce a smooth continuous function describing the free energy landscape for use in the Cahn-Hilliard equation. The polynomial used and its coefficients are reported in Table A2. This energy surface provides the free energies of Cr and Ni as a function of their local concentrations, which is necessary as an input for the Cahn-Hilliard model. These values are tabulated in Tables A3 and A4 and summarized in Figure 2. It is important to note that Thermo-Calc only calculates free energies for equilibrium phases, and it may be that the phase changes leading to SCC occur through non-equilibrium processes.

In addition to free energy values for Ni and Cr, the mobilities of Ni and Cr in our steel are important inputs to the Cahn-Hilliard model. Due to a limitation in how the Cahn-Hilliard equation is implemented in MOOSE, the mobility of each species was fixed for each simulation. This is nonphysical since a species' mobility depends on its chemical potential, which itself depends on an evolving local composition.

Code written for the final design is hosted on GitHub at:

<https://github.com/CriticalMoose/TestingMoose/>

Testing

By taking the most promising compositions from our simulations and running them through an accelerated testing environment with high temperature and neutron radiation it would have been possible to begin exploring whether or not simulations led to real materials results. Once the metals had been through annealing and radiation, we could perform a variety of tests on them, such as tensile testing, K1C fracture testing, corrosion testing, density change, and anisotropic swelling, to see how they have changed. Most importantly, we could also run a test to determine the SCC resistance of our new alloys [5]. There is a strong need for efforts that combine both simulation and experiment in materials research.

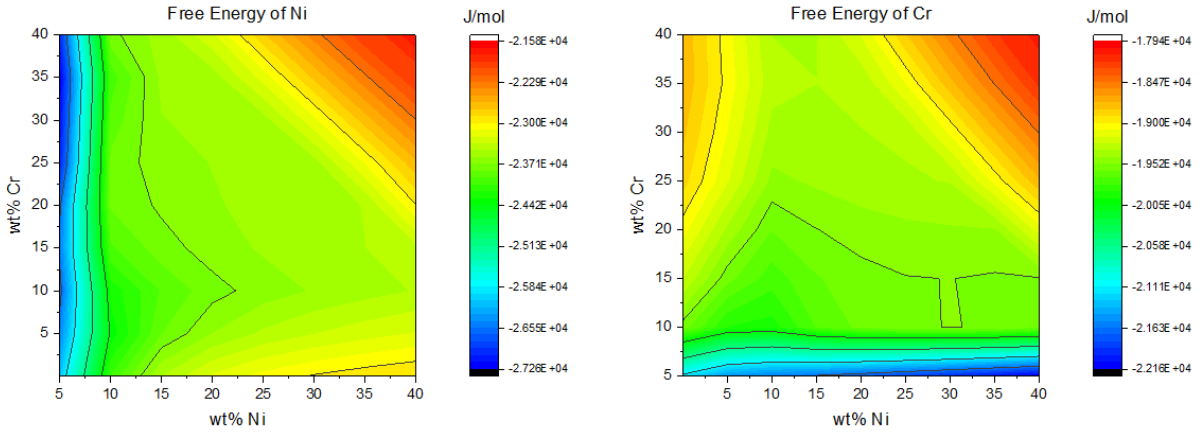


Figure 2: Free energy contour maps for Ni and Cr in 304L stainless steel generated from data obtained via ThermoCalc. The Ni and Cr compositions which yielded these maps ranged from 0.01 (approximating zero) to 40 wt% in 5 wt% increments. The Fe content was allowed to change as Ni and Cr concentrations were changed, while minor alloy additions such as Mn and Mo were kept constant.

Simulation on its own can not fully capture the physics of a certain situation, whereas experimentation on its own can often lead to results by tedious trial and error. An example of our simulation results is shown in Figure 3.

After running many simulations with the polynomial function for species free energy derived from Thermo-Calc data, it was found that the lack of cross terms between Ni and Cr concentration yielded non-physical results. The final distribution of Ni was unaffected by the Cr concentration of the alloy, and vice versa. The fitting algorithm used to produce this polynomial could not calculate cross terms, so we attempted to find values for these cross terms using an optimizing genetic algorithm.

In this algorithm a population of candidate function coefficients was randomly generated with the non-cross-terms sourced from the original polynomial fit to decrease the search time. The fitness of a candidate was determined by least squares regression compared to the data collected from Thermo-Calc over the entire composition range. At each generation, candidates with fitnesses below the mean were eliminated from the population and new candidates were generated by randomly combining and tweaking the coefficients from the remaining members of the population. This process was repeated until around 1,000 generations were produced. The candidate with the highest fitness was selected as the optimal set of coefficients.

While this new function improved the free energy function's R^2 value from 0.947 to 0.982, it also destabilized the simulation. Small fluctuations in composition exploded into discontinuities which ground the simulation to a halt; as seen in Figure 4, the composition in a small region oscillated between -3 and 1.5. This non-physical result led us to abandon our pursuit of cross terms for the free energy function.

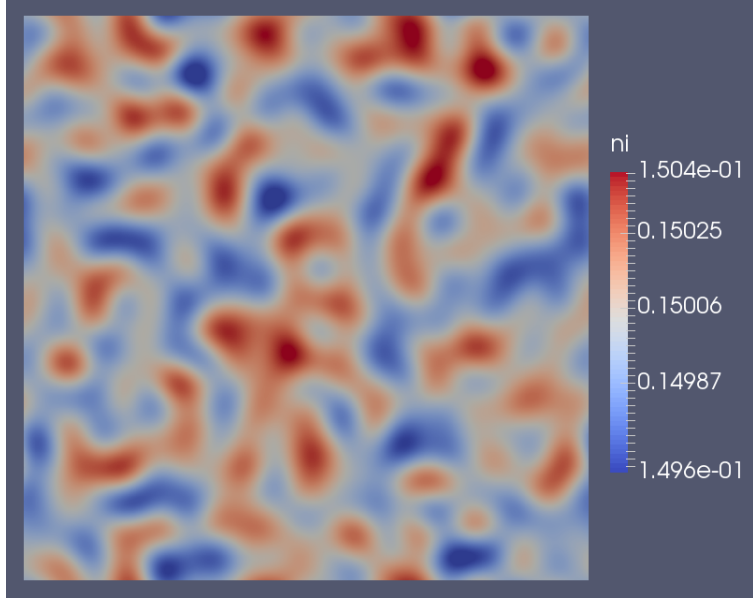


Figure 3: A representative final distribution of Ni in the alloy after 100 years simulated time. The distribution of Cr is very similar. The region is $250\mu\text{m} \times 250\mu\text{m}$ and the color bar has units of atomic fraction.

Benchmarking

304L type stainless steel was an obvious choice for a benchmark. It is a material currently used for many reactor core shrouds and is well documented in literature [3, 6, 7, 8]. The viability of alternate steels can be easily tested by comparing their phase field evolution to that of 304L. Whichever better maintains its chemical distribution and microstructure is considered superior. This avenue of proving requires a very reliable simulation package.

Another beneficial comparison would be to benchmark against pure Ni to evaluate radiation resistance, as Ni is well known to swell excessively under neutron radiation [9]. Setting a benchmark that we know will fail can yield useful results, as it can tell us what to look for in the simulation that would indicate poor radiation performance. Once we know what simulation outputs suggest radiation damage, we could look for these pointers in other alloys we test in the future. Neutron radiation damage could not be implemented in our final design, so this benchmark was not performed.

With the current state of our simulation, it is difficult to benchmark against the real resulting microstructure of a material used inside a nuclear reactor. Therefore in order to help assess the quality of our design we can compare our simulation results over the range of compositions which have been tested. Looking at the Ni versus Cr concentration of the different simulated compositions, it can be determined right away that some modifications to the final design must be made in order to accurately simulate the material changes over time in nuclear environments. Consequently, the overall design of our simulation has some shortcomings that should be mentioned in order to understand how our design would have fallen short compared to physical results.

The combination of effects (SCC, irradiation, grain growth, chemical segregation/phase

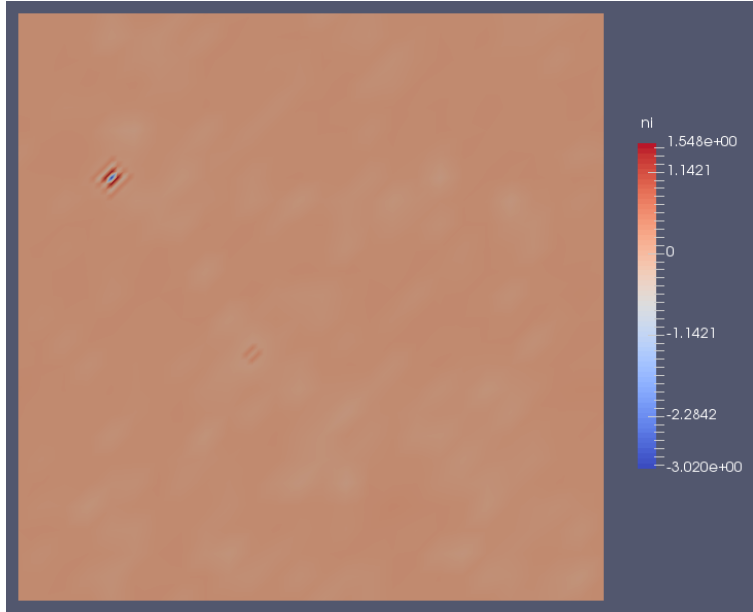


Figure 4: The distribution of Ni after several time steps using the free energy function with cross terms generated via an optimizing genetic algorithm. The concentration varies between -3 and 1.5 over a small area; this non-physical result led us to halt our pursuit of cross terms for the free energy function. The region is $250\mu\text{m} \times 250\mu\text{m}$ and the color bar has units of atomic fraction.

decomposition) could not be satisfactorily co-implemented. The obvious solution is to either figure out how to combine MOOSE modules to run in parallel with each other or build our own simulation module that implements a physics model other than Cahn-Hilliard. The latter is likely a more powerful approach, but would require much more work.

We were unable to determine non-equilibrium values for free energy as a function of composition. This is important since it cannot be assumed that there is chemical equilibrium in the steel after intense neutron radiation. A method for determining the free energies from experimental values may be more appropriate [7]. After the above point is clarified, the resulting fit needs to be tuned. One simple fix is that cross terms should be implemented, such as Ni-Cr instead of just Ni-Ni or Cr-Cr. Our own efforts to produce these cross terms via an optimizing genetic algorithm were unsuccessful.

Even if proper microstructures were included in simulation, it is not clear how this would influence mechanical properties, lifetime, etc. in a quantitative way. The best way to test mechanical properties is still to produce a sample with the same microstructure and perform mechanical tests. Additionally, the HAZ of a weld has a unique microstructure compared to the base metal or the weldment. These different initial conditions may significantly change the response to temperature, vacancy addition, and pressure over time.

References

- [1] M. Tonks, D. Gaston, P. Millett, D. Andrs, P. Talbot, "An object-oriented finite element framework for multiphysics phase field simulations", Computational Materials Science 51 (2012), p20-29.
- [2] J. Medoff, "Status Report: Intergranular Stress Corrosion Cracking of BWR Core Shrouds and Other Internal Components", U.S. Nuclear Regulatory Commission, Office of Nuclear Reactor Regulation, Division of Engineering (March 1996).
- [3] J. Kwon, A. Motta, "Radiation Hardening in BWR Core Shrouds: Relative Roles of Neutron and Gamma Irradiation", Reactor Dosimetry (2000), ASTM STP 1398
- [4] Y. Saito, "Computer Simulation of Spinodal Decomposition in Duplex Stainless Steels", Materials Science Forum (2012), Vols. 706-709, p1509-1514.
- [5] T. Terachi, T. Yamada, T. Miyamoto, K. Arioka, "SCC growth behaviors of austenitic stainless steels in simulated PWR primary water", Journal of Nuclear Materials 426 (2012), p59-70.
- [6] K.G. Field, Y. Yang, T.R. Allen, J.T. Busby, "Defect sink characteristics of specific grain boundary types in 304 stainless steel under high dose neutron environments", Acta Materialia 89 (2015), p438-449.
- [7] T.R. Allen, G.S. Was, "Modeling Radiation-Induced Segregation in Austenitic Fe-Cr-Ni Alloys", Acta Materialia 46 (1998), p3679-3691.
- [8] L. Tan, R.E. Stoller, K.G. Field, Y. Yang, H. Nam, D. Morgan, B.D. Wirth, M.N. Gussey, J.T. Busby, "Microstructural Evolution of Type 304 and 316 Stainless Steels Under Neutron Irradiation at LWR Relevant Conditions", JOM 68 (2016), No. 2, p517-529.
- [9] N.I. Budylkin, E.G. Mironova, V.M. Chernov a, Krasnoselov, S.I. Porollo, F.A. Garner. "Neutron-induced swelling and embrittlement of pure iron and pure Ni irradiated in the BN-350 and BOR-60 fast reactors". Journal of Nuclear Materials 375 (2008) 359–364.

Appendix

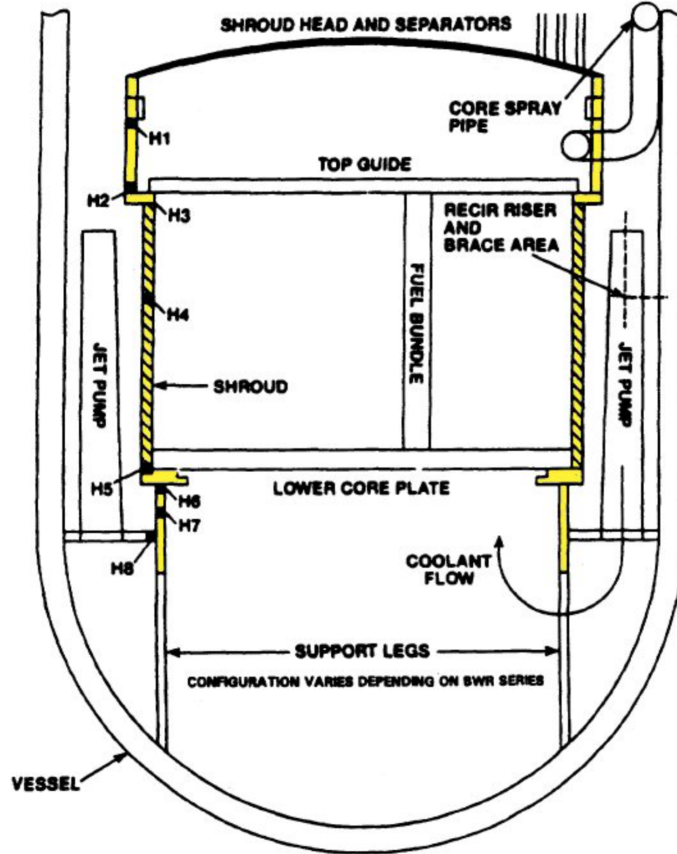


Figure A1: The yellow highlighted section shows the location of the core shroud within the reactor vessel. H1, H2, H3, etc., show locations of welds along the core shroud. These weld locations were found to be susceptible to SCC. Adapted from [2].

Table A1: Alloy composition used in the MOOSE simulation. Ni and Cr values were incremented by 5 wt%. All values given in weight percent.

Ni	Cr	Si	Mn	C	Mo	Fe
1-30	1-40	0.53	1.82	0.023	0.53	Bal.

Table A2: Coefficients of the polynomial used as the free energy function for the Cahn-Hilliard equation. The polynomial was of the form $z = z_0 + Ax + Bx^2 + Cx^3 + Dx^4 + Ex^5 + Fy + Gy^2 + Hy^3 + Iy^4 + Jy^5$ where x and y are the weight percent of Ni and Cr, respectively. The units of each coefficient are such that the sum has units of J/mol.

	z_0	A	B	C	D	E	F	G	H	I	J
Ni	-3.52e4	2690	-237	9.99	-0.201	1.56e-3	-125	11.3	-42.4	7.14e-3	-3.88e-5
Cr	-2.86e4	-86.8	4.22	-0.019	-2.15e-3	3.44e-5	2280	-210	9.22	-0.191	1.51e-3

Table A3: The free energy of Ni at various alloy compositions as calculated using Thermo-Calc. All values given in J/mol.

wt% Ni	wt% Cr	0.01	5	10	15	20	25	30	35	40
		0.01	5	10	15	20	25	30	35	40
0.01	0.01	-55547	-55901	-56100	-55943	-56050	-56493	-56612	-56728	-56446
	5	-26100	-26447	-26641	-26494	-26596	-27015	-27130	-27241	-26971
	10	-24059	-24376	-24259	-23965	-23814	-23797	-23907	-24013	-23755
	15	-23469	-23833	-23932	-23766	-23686	-23642	-23597	-23564	-23533
	20	-23213	-23588	-23759	-23651	-23606	-23587	-23556	-23532	-23261
	25	-23074	-23448	-23654	-23575	-23550	-23547	-23525	-23187	-22785
	30	-22987	-23355	-23580	-23519	-23508	-23517	-23148	-22735	-22348
	35	-22926	-23286	-23521	-23474	-23470	-23108	-22704	-22318	-21951
	40	-22878	-23227	-23466	-23386	-23007	-22672	-22295	-21936	-21590

Table A4: The free energy of Cr at various alloy compositions as calculated using Thermo-Calc. All values given in J/mol.

wt% Ni	wt% Cr	0.01	5	10	15	20	25	30	35	40
		0.01	5	10	15	20	25	30	35	40
0.01	0.01	-49877	-21168	-19568	-19254	-19046	-18870	-18799	-18751	-18752
	5	-50186	-21491	-19879	-19578	-19365	-19161	-19084	-19029	-19047
	10	-50350	-21588	-19912	-19746	-19607	-19459	-19376	-19314	-19348
	15	-50535	-21659	-19693	-19619	-19525	-19418	-19376	-19346	-19352
	20	-50732	-21749	-19588	-19556	-19480	-19382	-19349	-19325	-19162
	25	-50926	-21848	-19537	-19527	-19455	-19358	-19330	-19081	-18826
	30	-51114	-21950	-19519	-19521	-19444	-19342	-19064	-18761	-18514
	35	-51295	-22055	-19532	-19534	-19442	-19055	-18751	-18462	-18225
	40	-51468	-22158	-19582	-19530	-19124	-18748	-18459	-18184	-17958